

## Characterization of SCR Catalyst Based Ag-Nb-Pt

Ali KESKİN<sup>1</sup>, Abdulkadir YAŞAR\*<sup>2</sup>, Zeycan KESKİN<sup>3</sup>, M. Atakan AKAR<sup>1</sup>,  
İ. Aslan REŞİTOĞLU<sup>4</sup>, Himmet ÖZARSLAN<sup>1</sup>, Kadir AYDIN<sup>1</sup>

<sup>1</sup>Çukurova Üniversitesi, Mühendislik Fakültesi, Otomotiv Mühendisliği Bölümü, Adana

<sup>2</sup>Çukurova Üniversitesi, Ceyhan Mühendislik Fakültesi, Makine Mühendisliği Bölümü, Adana

<sup>3</sup>Mersin Üniversitesi, Tarsus Teknoloji Fakültesi, İmalat Mühendisliği Bölümü, Mersin

<sup>4</sup>Mersin Üniversitesi, Teknik Bilimler Meslek Yüksekokulu, Otomotiv Teknolojisi, Mersin

Geliş tarihi: 07.06.2018

Kabul tarihi: 25.12.2018

### Abstract

Selective Catalytic Reduction (SCR) is an emission control system used in diesel engines to reduce NO<sub>x</sub> emissions. In this study, synthesized of catalyst for SCR system was investigated as experimentally. For this purpose, silver nitrate (AgNO<sub>3</sub>), niobium (V) chloride (NbCl<sub>5</sub>) and tetra amine platinum (II) nitrate (Pt(NH<sub>3</sub>)<sub>4</sub>(NO<sub>3</sub>)<sub>2</sub>) were used to coat the cordierite (2Al<sub>2</sub>O<sub>3</sub>-5SiO<sub>2</sub>-2MgO) structure with impregnation method. X-ray Fluorescence (XRF), Scanning Electron Microscope (SEM) and Brunauer, Emmett, and Teller (BET) analyzes were carried out in order to determine the chemical and physical properties of the catalyst. Results showed that the coating materials penetrate the entire surface of the pores. It was also determined that the BET specific surface areas of the produced catalyst and cordierite are 0.2918 m<sup>2</sup>/g and 0.4568 m<sup>2</sup>/g, respectively. The reduction of surface area could be attributed to the increment of crystallization with chemical reactions occurred at the high sintering temperature. Besides, XRF analysis results demonstrated that content of Ag, Pt and Nb in the in the catalyst was found to be 3.67%, 0.19% and 0.12%, respectively, whereas Ag content in cordierite structure was 0.03%.

**Keywords:** Catalyst, XRF, SEM, BET, SCR, Exhaust emissions

### Ag-Nb-Pt Bazlı SCR Katalizör Karakterizasyonu

#### Öz

Seçici Katalitik İndirgeme (SCR), dizel motorlarda NO<sub>x</sub> emisyonlarını azaltmak için kullanılan bir emisyon kontrol sistemidir. Bu çalışmada, SCR sistemi için gümüş esaslı katalizörün sentezlenmesi deneysel olarak incelenmiştir. Bu amaçla, kordiyerit (2Al<sub>2</sub>O<sub>3</sub>-5SiO<sub>2</sub>-2MgO) yapısını daldırma yöntemiyle kaplamak amacıyla gümüş nitrat (AgNO<sub>3</sub>), niyobyum (V) klorür (NbCl<sub>5</sub>) ve tetra amin platin (II) nitrat (Pt (NH<sub>3</sub>)<sub>4</sub> (NO<sub>3</sub>)<sub>2</sub>) katalizörleri kullanılmıştır. Katalizörün kimyasal ve fiziksel özelliklerini belirlemek için XRF, SEM ve BET analizleri gerçekleştirilmiştir. Sonuçlar, kaplama malzemelerinin gözeneklerin tüm yüzeyine nüfuz ettiğini göstermiştir. Üretilen katalizör ve kordiyeritin BET yüzey alanlarının sırasıyla 0,2918 m<sup>2</sup>/g ve 0,4568 m<sup>2</sup>/g olduğu belirlenmiştir. Yüzey alandaki azalmanın, yüksek sinterleme sıcaklığında meydana gelen kimyasal reaksiyonlarla kristalizasyon artışına bağlı olduğu düşünülmektedir. Ayrıca, XRF analizi

\* Sorumlu yazar (Corresponding author): Abdulkadir YAŞAR, [ayasar@cu.edu.tr](mailto:ayasar@cu.edu.tr)

sonuçları, kordierit yapısındaki Ag içeriğinin %0,03 olmasına karşın katalizörde Ag, Pt ve Nb içeriğinin sırasıyla %3,67, %0,19 ve %0,12 oranlarında olduğunu ortaya koymuştur.

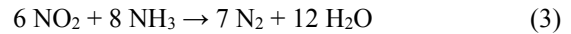
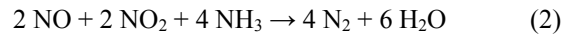
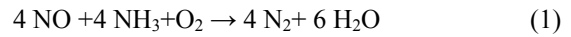
**Anahtar Kelimeler:** Katalizör, XRF, SEM, BET, SCR, Egzoz emisyonları

## 1. INTRODUCTION

NO<sub>x</sub> emissions deriving from NO and NO<sub>2</sub> forms are a contaminant emission type that can cause negative impacts on the environment and human health worldwide [1]. Acid rains are the most important factor of these negative effects [2].

A significant portion of NO<sub>x</sub> emissions comes from the transport sector. Compared to other types of vehicles, diesel-powered vehicles used in the transportation sector have the largest share of NO<sub>x</sub> emissions [3]. The high combustion temperature in diesel engines and the high air excess coefficient of diesel engines are the main factors in the formation of these emissions. In the event of a sufficient amount of oxygen in the environment above the 1600 °C temperature, NO<sub>x</sub> emissions consist of the result of N<sub>2</sub> and O<sub>2</sub> reactions [1]. Many research activities have been carried out to reduce NO<sub>x</sub> emissions from diesel engines. Exhaust Gas Recirculation (EGR) is a system developed for this purpose and widely used in modern vehicles [4]. In this system, a certain amount of exhaust gas is cooled and sent back into the cylinder and thus, the combustion temperature is reduced. Although this situation provides some reduction in NO<sub>x</sub> emissions, smoke, CO and HC emissions are adversely affected and an increase in these emissions is observed. Besides, a decrease in combustion efficiency may adversely affect engine performance [5]. Owing to these disadvantages, the interest in the EGR system is gradually decreasing day by day. Apart from the EGR system, the improvement of fuel properties using fuel additives, developing fuel injection systems and controlling engine operating parameters are also effective in reduction of NO<sub>x</sub> emissions [6-7]. However, these efforts have not provided a reduction that can meet the NO<sub>x</sub> emission values stated in the standards such as EURO, EPA and IPCC. The SCR system was developed as one of an engine emission control systems and has become widespread nowadays. It

provides the desired reductions in NO<sub>x</sub> emissions. In this system, NO<sub>x</sub> emissions can be reduced by chemical reactions in the presence of a catalyst together with a reductive sprayed into the exhaust gas [8-9]. Ammonia (NH<sub>3</sub>) is the most commonly used reductive in SCR systems. Due to the sudden burning of ammonia at high temperatures, the aqueous urea solution called AdBlue have been sprayed on the exhaust gas [10]. NO<sub>x</sub> emissions are removed from exhaust gas via the chemical reactions that occur in SCR catalyst. Base reactions for SCR are shown below.



Equation 1 is called as standard SCR reaction where the ratio of NH<sub>3</sub> and NO is 1:1. Equation 2 is referred to as fast SCR reaction due to its 1:1 of NO:NO<sub>2</sub> ratio. Equation 3 is known as slow SCR reaction where pure NO<sub>2</sub> takes place in the reaction. The conventional nanoparticles could gather easily during the catalytic process, leading to catalytic activity reduction. The ordered mesoporous materials having large surface-to-volume ratios and uniform porous structure show many interesting properties in catalysis, energy conversion and storage due to the fact that they have d-shell electrons held to nanosized walls, redox active internal surfaces compared to the nanoparticles, [11,12].

V<sub>2</sub>O<sub>5</sub>-WO<sub>3</sub>/TiO<sub>2</sub> is the most commonly used catalyst species in SCR systems [13]. However, this catalyst does not perform very well at low exhaust gas temperatures, and at the same time it can cause negative effects on the environment and human health due to the toxic effect of vanadium. In previous studies, many different materials (CeO<sub>2</sub>-TiO<sub>2</sub>, Cu /Al<sub>2</sub>O<sub>3</sub>, NbCe, Fe-MFI, Fe-ZSM<sub>5</sub>, Cu-ZSM<sub>5</sub>, Ag/Al<sub>2</sub>O<sub>3</sub>) have been tested as catalyst

by researchers for SCR systems [14]. Kim et al [15] revealed that Ag based catalyst promoted the oxidation of  $\text{NH}_3$  to  $\text{N}_2$ , while enhancing the  $\text{NO}_x$  performance of the conventional HC-SCR, especially at low temperatures. Pang et al [16] examined the  $\text{NH}_3$ -SCR activity on  $\text{V}_2\text{O}_5/\text{WO}_3\text{-TiO}_2$  catalysts prepared using the conventional impregnation methods. Kang et al [17] reported that manganese oxides with small amounts of copper oxide having high surface area were the most effective catalyst for low temperature NO reduction with  $\text{NH}_3$  in the availability of  $\text{SO}_2$ . Wu et al [18] studied Mn/TiO<sub>2</sub> doped with Ce which leads the resistance to  $\text{SO}_2$ . It was revealed that Ce addition significantly inhibit the formation of  $\text{Ti}(\text{SO}_4)_2$  and  $\text{Mn}(\text{SO}_4)_2$ . It was also demonstrated that amount of copper species had considerable effect on catalytic performance for Cu-containing SCR catalysts [19].

Many studies were conducted by researchers above mentioned. But there are still gap to understand the nature of Ag based SCR catalyst. Such understanding is especially necessary to establish suitable catalyst production process. The aim of the present study is to investigate the characterization of the Ag based SCR catalyst. In SCR catalyst production process, a lot of chemical matter such as silver nitrate ( $\text{AgNO}_3$ ), niobium (V) chloride ( $\text{NbCl}_5$ ) and tetraamine platinum (II) nitrate ( $\text{Pt}(\text{NH}_3)_4(\text{NO}_3)_2$ ) were used. These nano particles were utilized in order to coat on the cordierite structure ( $2\text{Al}_2\text{O}_3\text{-5SiO}_2\text{-2MgO}$ ). Furthermore, the characterization of catalyst was determined by XRF, BET and SEM analyzes.

## 2. MATERYAL VE METHOD

### 2.1. Catalyst Preparation

The catalyst samples were prepared by an impregnation method. In order to get samples, a solution was prepared composing of 30 g  $\text{AgNO}_3$ , 2g  $\text{NbCl}_5$  and 1g  $\text{Pt}(\text{NH}_3)_4(\text{NO}_3)_2$  nano particles. These nano particles were mixed in 500 ml distilled water via ultrasonic mixer for 20 minutes at room temperature. The carrier structure (cordierite) was dried at 110 °C for 2 h. The cordierite was immersed into the formed solution and was dried at 110 °C for 2 h. The same procedure was repeated for coated

cordierite structure. After impregnation process, drying and sintering processes were implemented with 110 °C for 2 h and 550 °C for 5 h, respectively. Finally, the catalyst samples for SEM/EDX, XRF and BET analyzing were prepared in order to determine characterization of the catalyst. Flowchart of catalyst production is given in Figure 1.

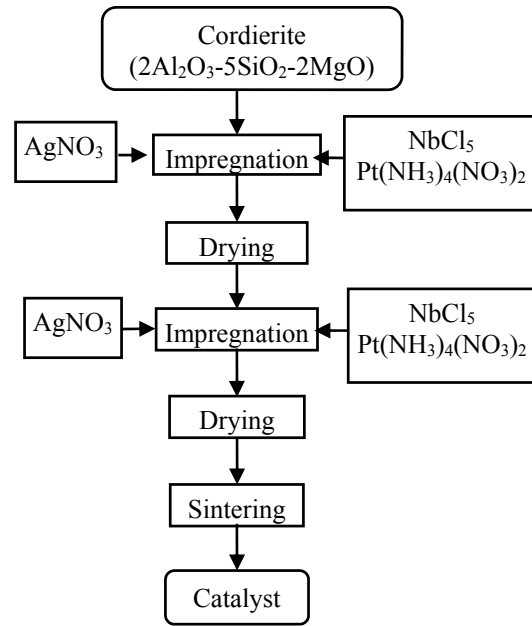


Figure 1. Flow chart of catalyst production

### 2.2. Catalyst Characterization

SEM analysis of cordierite and synthesized catalyst was performed at Cukurova University Central Research Laboratory (Cumerlab). The device used is Quanta FEG 650 having enlargements of 6-1.000.000x. In order to examine non-conductive samples, the samples was coated with conductive material at a thickness of about 2 Å/sec. Qualitative and quantitative elemental analyzes was performed on the sample using the EDX spectrometer in the instrument. Surface area analysis was conducted using the Micromeritics TriStar II device in Kahramanmaras Sutcu Imam University, USKIM. The surface area was calculated by determining the area covered by a single gas molecule adsorbed to the surface and finding the total number of

molecules adsorbed on the surface. Brunauer-Emmett-Teller method was used in these calculations. Bruker S8 Tiger device located at Kahramanmaraş Sutcu Imam University, USKIM was utilized for XRF analysis which give information on the type of elements contained in the samples and the concentration of these elements.

The catalyst sample was pulverized using a grinder to perform XRF and BET analysis. 10 g of the powder sample was mixed with cellulose of 4 g and the prepared mixture was compressed at 36 MPa pressure and pelletized to use in XRF analysis. BET surface area analysis was performed using nitrogen gas at a temperature of -196 °C.

### 3. RESULTS AND DISCUSSION

#### 3.1. BET Surface Area Results

The BET data for the cordierite structure and produced catalyst are given in Table 1. The N<sub>2</sub>

adsorption-desorption isotherms of Ag-Nb-Pt catalyst and cordierite are shown in Figure 2. The BET specific surface areas of produced catalyst and cordierite are about 0.2918 m<sup>2</sup>/g and 0.4568 m<sup>2</sup>/g, respectively. Compared with the cordierite main structure, a reduction of 36.12% in the surface area of the catalyst produced was observed.

Sintering process of the catalyst can be shown as the main reason for the reduction in surface area due to chemical reactions which could increase formation of the metallic particle crystallization. These reactions caused formation of new structures on surface of cordierite. Accordingly, this case caused reduction on surface area of the catalyst. The average pore diameter of the cordierite structure was measured as 21.4072 nm, whereas this value was 54.4758 nm for the produced catalyst. While the cordierite structure was mezopored, it became macro porous after coating since the pore diameter exceeded 50 nm.

**Table 1.** BET analysis of cordierite and Ag-Nb-Pt catalyst

Summary Report	Cordierite	Ag-Nb-Pt
<i>Surface Area</i>		
BET Surface Area	0.4568 m <sup>2</sup> /g	0.2918 m <sup>2</sup> /g
Langmuir Surface Area	0.6105 m <sup>2</sup> /g	0.3800 m <sup>2</sup> /g
BJH adsorption cumulative surface area of pores between 17.000 Å and 3000.000 Å width	0.183 m <sup>2</sup> /g	0.063 m <sup>2</sup> /g
BJH desorption cumulative surface area of pores between 17.000 Å and 3000.000 Å width	0.1279 m <sup>2</sup> /g	0.0647 m <sup>2</sup> /g
<i>Pore Volume</i>		
BJH adsorption cumulative volume of pores between 17.000 Å and 3000.000 Å width	0.000981 cm <sup>3</sup> /g	0.000856 cm <sup>3</sup> /g
BJH desorption cumulative volume of pores between 17.000 Å and 3000.000 Å width	0.001106 cm <sup>3</sup> /g	0.000857 cm <sup>3</sup> /g
<i>Pore Size</i>		
Adsorption average pore width (4V/A by BET)	83.2510 Å	96.6573 Å
BJH Adsorption average pore width (4V/A)	214.072 Å	544.758 Å
BJH Desorption average pore width (4V/A)	345.889 Å	530.322 Å

Figures 2 and 3 show the variation of relative pressure and absolute pressure with quantity

adsorbed, respectively. In isotherm curves shown in Figures 2 and 3, adsorption amount of nitrogen gas

used for determining surface area and pore size distribution takes positive values at low relative pressures. However, as the relative pressure increases, the amount of adsorption decreases to negative values and again positive values at high relative pressure values are obtained. This is believed to be due to the low surface area of the synthesized catalyst. The reduction in surface area is achieved as a result of the reduced NO<sub>x</sub> reduction activity of the catalyst.

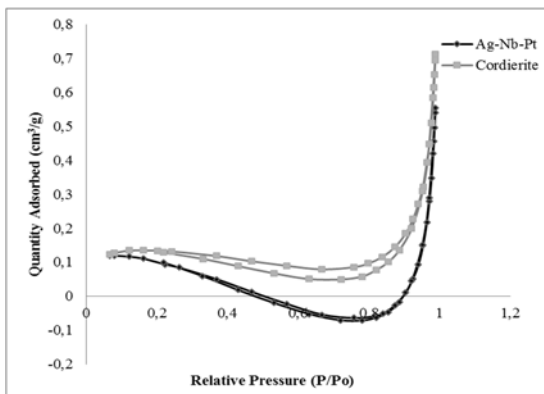


Figure 2. Variaton of relative pressure with quantity absorbed

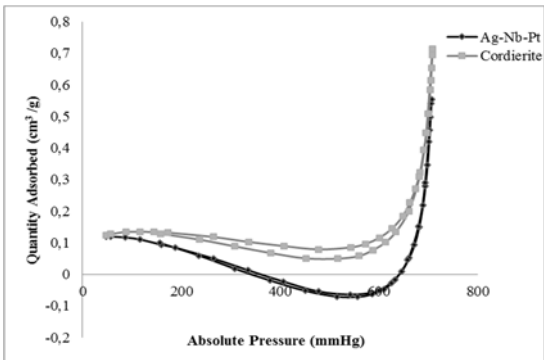


Figure 3. Variaton of absolute pressure with quantity absorbed

Variation of pore width with respect to pore volume is given Figure 4. As shown in Figure 4, pore volume decreases with the increase of pore width. Figure 5 shows the variation of pore width with pore area. As can be seen from Figure 5, when the pore width increases, pore surface area decreases. Eventually, as the pore width increases, the surface

area decreases and surface area increases with the increases of pore volume.

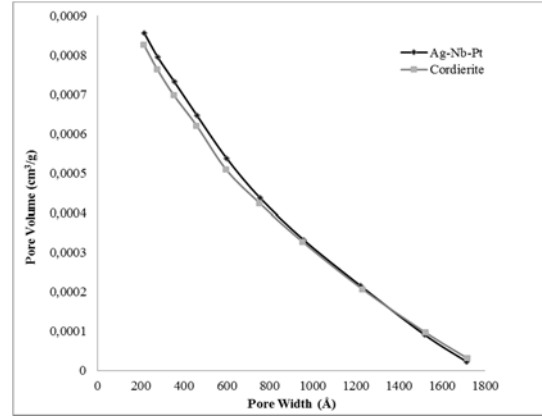


Figure 4. BJH adsorption cumulative pore volume (Larger) Halsey: Faas correction

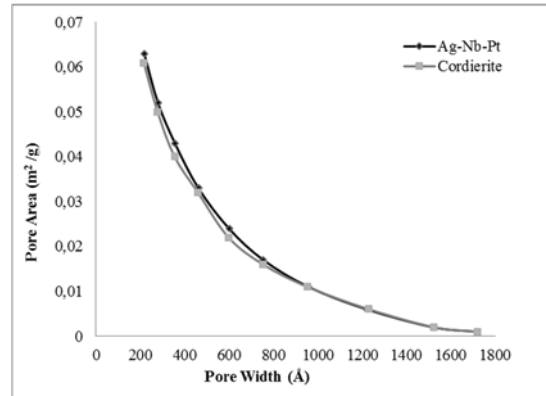


Figure 5. BJH adsorption cumulative pore area (Larger) Halsey: Faas correction

In general, the surface area of the catalysts is the most important factor affecting the catalytic activity. BET graphs were obtained with the determination of the adsorption capacities of cordierite and catalyst. These graphs were attained with the values of the relative equilibrium pressure in the range of 0.05-0.35. When the slope of BET increases, specific surface area decreases. BET surface area is given in Figure 6. As shown in Figure 6, the slope of the catalyst seems to be higher than that of the cordierite. This means that the specific surface area of the catalyst is less than that of the cordierite.

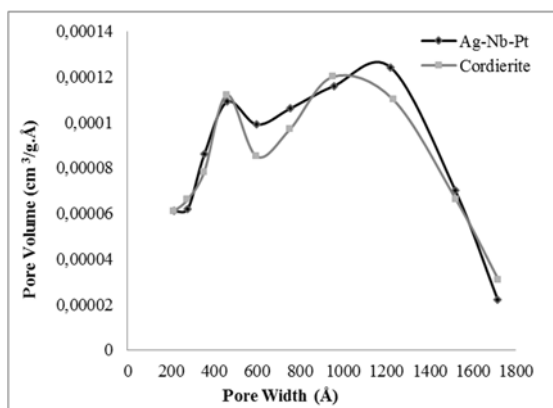


Figure 6. BET surface area plot

Figure 7 displays the variation of pore width with BJH adsorption  $dV/dw$  curve which allows the determination of pore volume. In Figure 7, it is seen that pore concentrations increase in pore width values between 10-50 nm for cordierite. This situation is resulted from the presence of mesoporous. In curve belonged to the catalyst, it was determined that pore concentrations decreased with increasing of pore width.

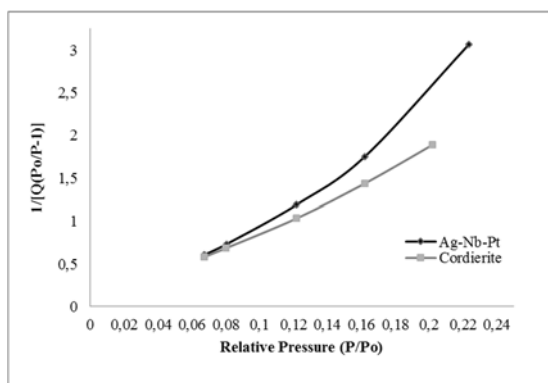


Figure 7. Pore size distribution

### 3.2. XRF Analysis Results

XRF analysis results of the cordierite structure and produced catalyst with the percentage of the elements and compounds in the sample contents are given in Table 2. According the results, the  $\text{SiO}_2$  and  $\text{Al}_2\text{O}_3$  compounds forming the main structure in the samples were obtained at the highest rate. When Ag content in the cordierite structure was 0.03%,

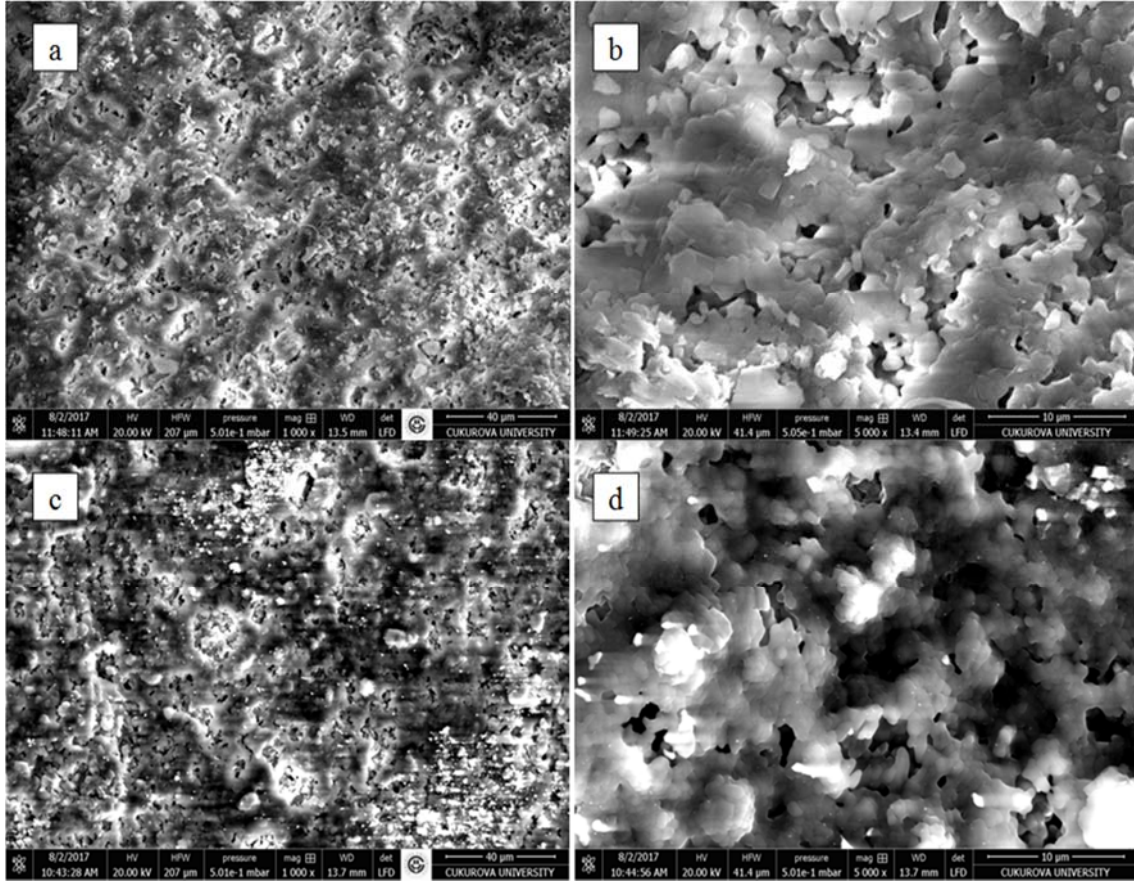
this ratio was found to be 3.67% in the catalyst. The Pt content in the catalyst is 0.19% and the Nb content is 0.12%.

Table 2. XRF analysis results

Cordierite		Ag-Nb-Pt	
69.50%		77.80%	
Formula	Concentr.	Formula	Concentr.
$\text{SiO}_2$	34.10%	$\text{SiO}_2$	35.78%
$\text{Al}_2\text{O}_3$	24.12%	$\text{Al}_2\text{O}_3$	25.96%
$\text{MgO}$	9.85%	$\text{MgO}$	10.63%
$\text{Fe}_2\text{O}_3$	0.42%	Ag	3.67%
$\text{P}_2\text{O}_5$	0.29%	$\text{Fe}_2\text{O}_3$	0.49%
CaO	0.19%	$\text{P}_2\text{O}_5$	0.29%
$\text{TiO}_2$	0.15%	CaO	0.21%
$\text{K}_2\text{O}$	0.11%	$\text{TiO}_2$	0.16%
PbO	0.06%	$\text{Na}_2\text{O}$	0.11%
$\text{ZrO}_2$	0.05%	$\text{K}_2\text{O}$	0.10%
$\text{Cr}_2\text{O}_3$	0.05%	Pt	0.09%
Ag	0.03%	$\text{Nb}_2\text{O}_5$	0.08%
$\text{SO}_3$	0.01%	$\text{Cr}_2\text{O}_3$	0.06%
NiO	0.01%	PbO	0.05%
		$\text{ZrO}_2$	0.04%
		$\text{SO}_3$	0.03%
		NiO	0.02%

### 3.3. SEM/EDX Analysis Results

The structure and morphology of the catalyst are very important parameters as they influence the photocatalytic activity. SEM images of 1000x and 5000x sizes of cordierite and produced catalysts are shown in Figure 8. When the SEM/EDX analysis results are examined, it is determined that the catalysts have a highly porous structure, the coating on the cordierite structure is homogeneous throughout the entire surface, and the coating materials penetrate the entire surface including the pores. In addition, the Ag based catalyst has higher crystallinity.



**Figure 8.** Images of SEM; a) Cordierite 1000x, b) Cordierite 5000x, c) Ag-Nb-Pt 1000x, d) Ag-Nb-Pt 5000x

#### 4. CONCLUSION

In this experimental study, it was aimed to develop and synthesize Ag, Nb and Pt catalysts for use in SCR system. The cordierite structure was immersed in the solution consisting of Ag, Nb and Pt elements and then dried and sintered at high temperature. BET, XRF and SEM/EDX analyzes of the developed catalyst were executed. As a result of the analysis, it was shown that the coating was performed homogeneously. In addition, the Ag, Nb and Pt admixtures penetrate the entire surface and the surface area of the catalyst has decreased due to the high temperature exposure. In further study, it is planned to investigate the effect on the emissions by connecting the produced catalyst to the outlet of an engine.

#### 5. REFERENCES

1. Resitoglu, I.A., Altınışık, K., Keskin A., 2015. The Pollutant Emissions from Diesel-engine Vehicles and Exhaust Aftertreatment Systems. *Clean Tech. Environ.* 17, 15-27.
2. Bell, J.N.B., Honour, S.L., Power, S.A., 2011. Effects of Vehicle Exhaust Emissions on Urban Wild Plant Species. *Environ. Pollut.* 159, 1984-1990.
3. Lee, T., Park, J., Kwon, S., Lee, J., Kim, J., 2013. Variability in Operation-based NO<sub>x</sub> Emission Factors with Different Test Routes, and its Effects on the Real-driving Emissions of Light Diesel Vehicles. *Sci. Total Environ.* 461-462, 377-385.

4. Guan, W., Pedrozo, V., Zhao, H., Ban, Z., Lin, T., 2017. Investigation of EGR and Miller Cycle for NO<sub>x</sub> Emissions and Exhaust Temperature Control of a Heavy-Duty Diesel Engine. SAE Tech. Paper. 01, 2227.
5. Wu, H.W., Hsu, T.T., He, J.Y., Fan, C.M., 2017. Optimal Performance and Emissions of Diesel/hydrogen-rich Gas Engine Varying Intake Air Temperature and EGR Ratio. Appl. Therm. Eng. 124, 381-392.
6. Johnson, T.V. 2009. Review of Diesel Emissions and Control. Int. J. Eng. Res. 10(5), 275-285.
7. Kalam, M.A., Masjuki, H.H., 2008. Testing Palm Biodiesel and NPAA Additives to Control NO<sub>x</sub> and CO While Improving Efficiency in Diesel Engines. Biomass and Bioener. 32(12), 1116-1122.
8. Resitoglu, I.A., Keskin, A., 2017. Hydrogen Applications in Selective Catalytic Reduction of NO<sub>x</sub> Emissions from Diesel Engines. Int. J. Hydr. Ener. 42(36), 23389-23394.
9. Ingole, A.K., Dixit, D., Dingare, S.V., 2017. A Review on Selective Catalytic Reduction Technique for Diesel Engine Exhaust After Treatment. Int. J. Curr. Eng. Tech. 7, 206-210.
10. Stanculescu, M., Charland, J.P., Kelly J.F. 2010. Effect of Primary Aminehydrocarbon Chain Length for the Selective Catalytic Reduction of NO<sub>x</sub> from Diesel Engine Exhaust. Fuel. 89, 2292-2298.
11. Jiao, F., Hill, A.H., Harrison, A., Berko, A., Chadwick, A.V., Bruce, P.G., 2008. Synthesis of Ordered Mesoporous NiO with Crystalline Walls and a Bimodal Pore Size Distribution. J. Am. Chem. Soc. 130, 5262-5266.
12. Zhang, Y., Zhao, X.C., Wang, Y., Zhou, L., Zhang, J., Wang, J., Wang, A., Zhang, T., 2013. Mesoporous Ti-W Oxide: Synthesis, Characterization and Performance in Selective Hydrogenolysis of Glycerol. J. Mater. Chem. A 1, 3724-3732.
13. Rauch, D., Albrecht, G., Kubinski, D., Moos, R., 2015. A Microwave-based Method to Monitor the Ammonia Loading of Vanadia-based SCR Catalyst. Appl. Catal. B: Environ. 165, 36-42.
14. Oliveira, M.L.M., Silva, C.M., Tost, R.M., Farias, T.L., Lopez, A.J., Castellon E.R., 2011. Modelling of NO<sub>x</sub> Emission Factors from Heavy and Light-duty Vehicles Equipped with Advanced Aftertreatment Systems. Ener. Conv. Manag. 52, 2945-2951.
15. Pang, L., Fan, C., Shao, L., Yi, J., Cai, X., Wang, J., Kang, M., Li, T., 2014. Effect of V<sub>2</sub>O<sub>5</sub>/WO<sub>3</sub>-TiO<sub>2</sub> Catalyst Preparation Method on NO<sub>x</sub> Removal from Diesel Exhaust. Chinese J. Catal. 35, 2020-2028.
16. Kim, P.S., Cho, B.K., Nam, I.S., Choung, J.W., 2016. Bifunctional Ag-based Catalyst for NO<sub>x</sub> Reduction with E-diesel Fuel. Chem Cat Chem. 6, 1570-1574.
17. Kang, M., Park, E.D., Kim, J.M., Yie, J.E., 2006. Cu-Mn Mixed Oxides for Low Temperature NO Reduction with NH<sub>3</sub>. Catal. Today. 111(3-4), 236-241.
18. Wu, Z., Jin, R., Wang, H., Liu, Y., 2009. Effect of Ceria Doping on SO<sub>2</sub> Resistance of Mn/TiO<sub>2</sub> for Selective Catalytic Reduction of NO with NH<sub>3</sub> at Low Temperature. Catal. Commun. 10, 935-939.
19. Kwak, J.H., Tonkyn, R., Tran, D., Mei, D., Cho, S.J., Kovarik, L., Lee, J.H., Peden, C.H.F., Szanyi, J., 2012. Size-Dependent Catalytic Performance of CuO on γ-Al<sub>2</sub>O<sub>3</sub>: NO Reduction versus NH<sub>3</sub> Oxidation ACS Catal. 2, 1432-1440.